DOI 10.5162/Ultrasonic2025/P1.21

Characterization of defects in aluminum plates using acoustic impedance analysis of piezoelectric ceramic discs

Mário Kyohi Takahasi[1], *Joaquim Miguel Maia*[1,2,3], *Wilson José da Silva*[1,3], *Amauri Amorin Assef*[1,4], *Rosalba da Costa*[4], *Sergio Francisco Pichorim*[1,3], *and Eduardo Tavares Costa*[5]
[1] *Graduate School of Electrical Engineering and Applied Computer Sciences (CPGEI), Federal University of Technology–Paraná (UTFPR), Curitiba, Brazil*
[2] *Graduate Program in Biomedical Engineering (PPGEB)*
[3] *Academic Department of Electronics Engineering (DAELN), UTFPR, Curitiba, Brazil*
[4] *Academic Department of Electrical Engineering (DAELT), UTFPR, Curitiba, Brazil*
[5] *Department of Electronics and Biomedical Engineering (DEEB), & Biomedical Engineering Centre (CEB), State University of Campinas (UNICAMP), Campinas, Brazil*
joaquim@utfpr.edu.br

Abstract: This work aimed to identify defects in aluminum plates by analyzing the module and phase angle of the electrical impedance of piezoelectric ceramics. Five aluminum plates with three centrally aligned holes in the center of the plate, and one reference plate (without holes) were used. Four ceramic discs were fixed to each of the six plates, and the impedances were compared using the root mean square deviation index (RMSD). The results showed that the method can be used for material characterization using the vibration modes of the ceramics.

Keywords: Piezoelectric ceramics, aluminum plates, electrical impedance, RMSD, material characterization.

Background, Motivation, and Objective

Piezoelectric ceramics coupled with different materials for defect evaluation offer a low-cost alternative for performing non-destructive tests (NDT) and material characterization to be applied in various areas, including biomedicine, the construction industry, naval, aeronautics, mechanical, physics, and others [1]–[7].

These kinds of NDT have been used for a long time and can still be innovative today. Some applications use the electrical impedance of piezoelectric ceramics [1]–[4]; the propagation of Lamb waves through the materials [8]–[10]; the instantaneous phase, attenuation, and speed of ultrasound waves measured using the pulse-echo or the transmission-reception methods [2], [5]–[7], [11], [12]; 2D and 3D images acquired using the B-mode scan; among others [7].

This work aimed to identify defects in aluminum square plates by analyzing the electrical impedance of piezoelectric ceramics coupled in different positions of these plates.

Materials and Methods

Six aluminum plates measuring 500 × 500 × 5 mm³ were used, one of which, without holes, was the reference plate. The others had three holes of the same diameter, aligned in the center of the plate, 250 mm from each side where the ceramics were placed and 125, 250, and 375 mm from the edges where there were no ceramics, simulating defects with 2, 4, 6, 8, and 10 mm in diameter. Four piezoelectric ceramic discs of APC 855 type (12.7 mm diameter and 2.0 mm thickness) were fixed to each of the six plates using conductive silver-based glue. The ceramics were all placed on the same side of the plate, one close to the bottom edge (centered at 250 mm – PR), and three close to the top edge (centered at 125 mm – P1, 250 mm – P2, and 375 mm – P3), as shown in Fig. 1(a). The module and phase angle of electrical impedance were measured in each ceramic disc on all the sample plates using an impedance analyzer (model 4294A, Agilent Technologies). Fig. 1(b) presents the block diagram of the setup used to measure the electrical impedance of each ceramic disc coupled to the sample plates.

The impedances were compared in three ranges (40 kHz to 1.3 MHz – all vibration modes, 150 kHz to 200 kHz – radial vibration mode, and 950 kHz to 1.3 MHz – axial vibration mode) using the root mean square deviation index (RMSD), as in Eq. (1) [4], where Zn,r is the impedance module in the reference plate, Zn,s is for the sample plate containing defects, n corresponds to the measurement obtained, and p (801 points) is the total number of measurements comprising the range of frequencies used in the impedance analyzer.

$$\mathrm{RMSD} = \sqrt{\frac{\sum_n^p (Z_{n,s} - Z_{n,r})^2}{\sum_n^p Z_{n,r}^2}} \qquad (1)$$

DOI 10.5162/Ultrasonic2025/P1.21

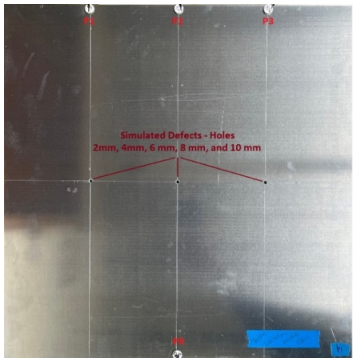

(a)

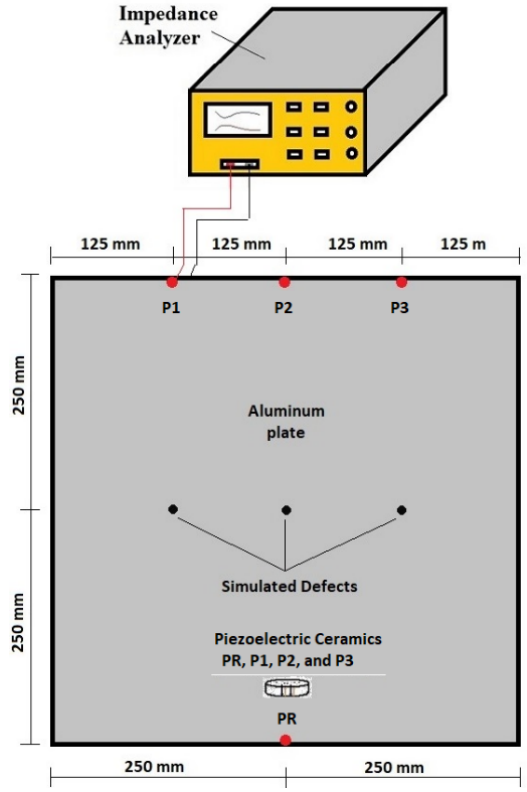

(b)

Fig. 1: (a) Sample plate with the ceramic discs APC 855 (12.7 mm × 2.0 mm) fixed using conductive silver-based glue; (b) Block diagram of the system used to measure the electrical impedance of the piezoelectric discs coupled to each of the six sample plates.

Results and Discussion

The module and phase angle of the electrical impedance obtained for a free APC 855 ceramic disc are shown in Fig. 2(a). It is possible to see all vibration modes in the frequency range of 40 kHz to 1.3 MHz. Fig. 2(b) shows the impedance modules for the six free ceramics before they were fixed in the position PR, see Fig. 1(b), of the aluminum plates, showing a similar module for all of them.

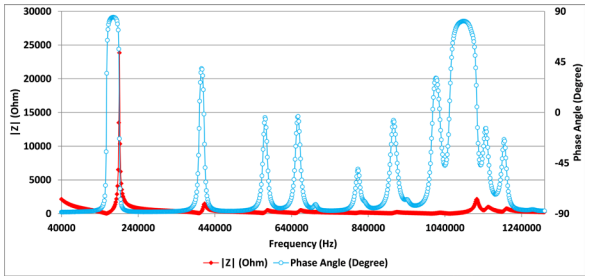

(a)

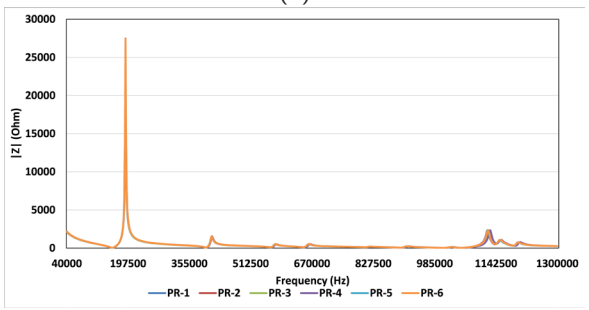

(b)

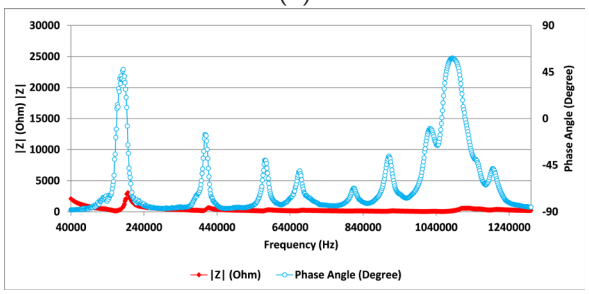

(c)

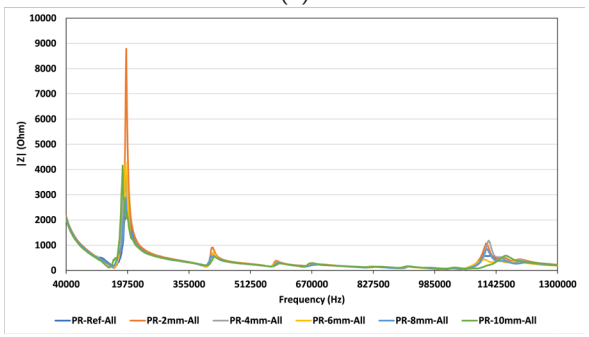

(d)

Fig. 2: (a) Electrical impedance for a free ceramic disc APC 855 showing a frequency range (40 kHz – 1.3 MHz) that includes all vibration modes; (b) Module of the impedance for all six free ceramics before they were fixed in the position PR of the six plates; (c) Electrical impedance for a fixed ceramic disc in the position PR, see Fig. 1(b), of the reference plate, showing the changes in the vibration mode when compared with the results shown in (a); (d) Impedance module for the six ceramics fixed in the six plates (the reference plate, and those with holes of 2, 4, 6, 8, and 10 mm).

DOI 10.5162/Ultrasonic2025/P1.21

When one of the ceramics was fixed in the position PR of the reference plate, changes in the vibration modes were observed, as shown in Fig. 2(c). Fig. 2(d) shows the changes for the impedance module after the six ceramics were coupled to the six aluminum plates (the reference plate and those with holes of 2, 4, 6, 8, and 10 mm). These kinds of changes were also observed in other studies [1]–[4].

Fig. 3(a) presents the impedance modules for the ceramics coupled to the six aluminum plates for the radial vibration mode (frequency range of 150 kHz – 200 kHz), and Fig. 3(b) presents the curves for the axial vibration mode (frequency range of 950 kHz – 1.3 MHz).

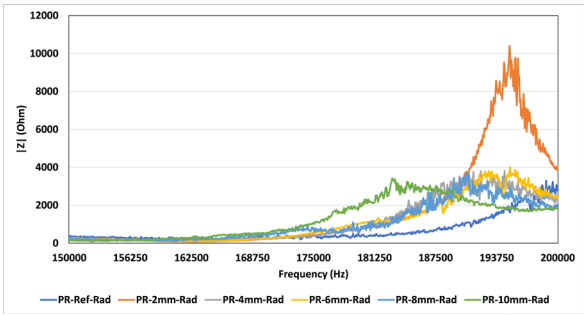

(a)

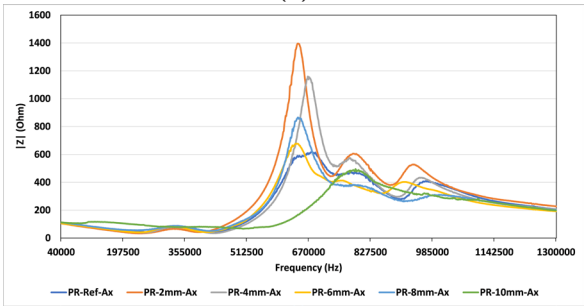

(b)

Fig. 3: Impedance module for the six ceramics fixed in the six plates (the reference plate, and those with holes of 2, 4, 6, 8, and 10 mm) for (a) the radial vibration mode in the frequency range of 150 kHz – 200 kHz, and (b) for the axial vibration mode in the frequency range of 950 kHz – 1.3 MHz.

The RMSD values obtained for the ceramics located in the PR position for the reference plate and the defective samples (with holes of 2, 4, 6, 8, and 10 mm) in the frequency range involving all vibration modes (40 kHz to 1.3 MHz) are shown in Fig. 4(a). The values for the radial vibration mode (150 kHz to 200 kHz) are shown in Fig. 4(b), and for the axial vibration mode (950 kHz to 1.3 MHz) in Fig. 4(c).

The RMSD results for the other ceramics at positions P1, P2, and P3 in all vibration modes (40 kHz to 1.3 MHz), radial modes (150 kHz to 200 kHz), and axial modes (950 kHz to 1.3 kHz) for the reference plate and the defective samples (with holes of 2, 4, 6, 8, and 10 mm) are shown in Tab. 1.

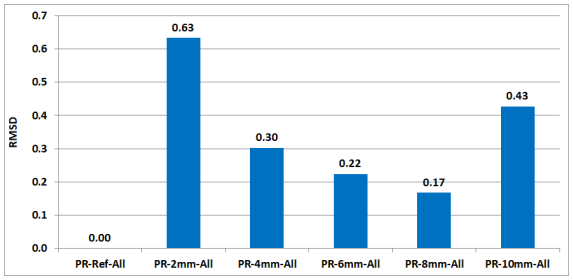

(a)

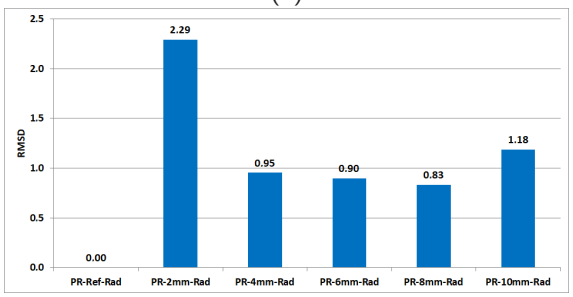

(b)

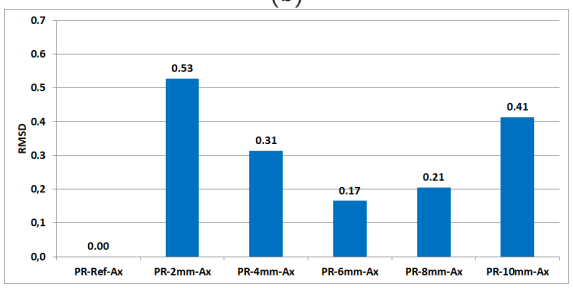

(c)

Fig. 4: RMSD values obtained for the ceramics located in the PR position for the reference plate and the defective samples (with holes of 2, 4, 6, 8, and 10 mm) in the frequency range involving (a) all vibration modes (40 kHz to 1.3 MHz), (b) the radial vibration mode (150 kHz to 200 kHz), and (c) the axial vibration mode (950 kHz to 1.3 MHz).

Conclusion

The results' analysis showed that the RMSD between the samples with defects and the reference sample can be used for material characterization using all the vibration modes of the ceramics or the radial and axial modes alone. Since the radial mode involves a lower frequency range, more straightforward and cost-effective electronic circuits can be designed to operate in this frequency range.

Tab. 1: RMSD values for the ceramics at positions P1, P2, and P3 (see Fig. 2) in all vibration modes (40 kHz to 1.3 MHz), radial mode (150 kHz to 200 kHz), and axial mode (950 kHz to 1.3 kHz) for the reference plate and the defective samples (with holes of 2, 4, 6, 8, and 10 mm).

Ceramics	Position	All modes	Radial mode	Axial mode
Reference	P1	0.00	0.00	0.00
	P2	0.00	0.00	0.00
	P3	0.00	0.00	0.00
2 mm holes	P1	0.20	0.19	0.39
	P2	0.25	0.54	0.66
	P3	0.19	0.51	0.29
4 mm holes	P1	0.26	0.20	0.31
	P2	0.24	0.23	0.78
	P3	0.33	0.41	0.27
6 mm holes	P1	0.63	0.88	0.73
	P2	0.39	0.66	0.79
	P3	0.34	0.72	0.28
8 mm holes	P1	0.52	0.58	0.37
	P2	0.44	0.31	0.49
	P3	0.16	0.34	0.29
10 mm holes	P1	0.29	0.66	0.18
	P2	0.48	0.85	0.41
	P3	0.34	0.95	0.76

Acknowledgements

The authors thank the Brazilian Coordination for the Improvement of Higher Education Personnel (CAPES), grant 001, the National Council for Scientific and Technological Development (CNPq), grant 408274/2021-2, the Federal University of Technology – Paraná (UTFPR), and the Araucaria Foundation for the financial support.

References

[1] P. Cawley, 'The impedance method of non-destructive inspection,' *NDT & E International*, vol. 17, pp. 59–65, 1984. DOI: 10.1016/0308-9126(84)90045-2.

[2] R. Costa and et al., 'Defect detection in aluminum bars using impedance and ultrasonic attenuation,' *IEEE Sensors Journal*, vol. 20, pp. 7400–7413, 2020. DOI: 10.1109/JSEN.2020.2978427.

[3] G. Park and et al., 'Impedance-based health monitoring technique for massive structures and high-temperature structures,' in *Smart Struct. and Mater. Proceedings of the SPIE*, vol. 3670, 1999, pp. 461–469. DOI: 10.1117/12.349760.

[4] X. Dongyu and et al., 'Identifying technology for structural damage based on the impedance analysis of piezoelectric sensor,' *Const. Build. Materials*, vol. 24, pp. 2522–2527, 2010. DOI: 10.1016/j.conbuildmat.2010.06.004.

[5] F. Lefebvre and et al., 'Development of a new ultrasonic technique for bone and biomaterials in vitro characterization,' *Biomed Mater Res*, vol. 63, pp. 441–6, 2002. DOI: 10.1002/jbm.10261.

[6] J. M. Maia and et al., 'Broadband ultrasound attenuation in the calcaneal region: A comparative study of single-position versus scanning systems,' *IEEE Trans. Ultras., Ferroel., and Freq. Control*, vol. 55, pp. 64–73, 2008. DOI: 10.1109/TUFFC.2008.617.

[7] F. Honarvar and A. Varvani-Farahami, 'A review of ultrasonic testing applications in additive manufacturing: Defect evaluation, material characterization, and process control,' *Ultrasonics*, vol. 108, 2020. DOI: 10.1016/j.ultras.2020.106227.

[8] Y. Lu and et al., 'Quantitative assessment of through-thickness crack size based on lamb wave scattering in aluminum plates,' *NDT & E International*, vol. 41, pp. 59–68, 2008. DOI: 10.1016/J.NDTEINT.2007.07.003.

[9] F. Benmeddour and et al., 'Study of the fundamental lamb modes interaction with asymmetrical discontinuities,' *NDT & E International*, vol. 41, pp. 330–340, 2008. DOI: 10.1016/j.ndteint.2008.01.004.

[10] Z. Su and et al., 'Guided lamb waves for identification of damage in composite structures: A review,' *J. of Sound and Vibration*, vol. 295, pp. 753–780, 2006. DOI: 10.1016/j.jsv.2006.01.020.

[11] V. T. Prado and et al., 'Defect detection in anisotropic plates based on the instantaneous phase of signals,' *IEEE Trans. Ultras., Ferroel., and Freq. Control*, vol. 62, pp. 1888–1894, 2015. DOI: 10.1109/TUFFC.2014.006955.

[12] R. C. Mayworm and et al., 'A metrological based realization of time-of-flight diffraction technique,' *Physics Procedia*, vol. 70, pp. 590–593, 2015. DOI: 10.1016/j.phpro.2015.08.029.